

A Charge-Transfer Reaction at the Electrified Tantalum-Pentoxide-Electrolyte Interface

Joachim Hossick-Schott and Mark. E. Viste

Medtronic Energy and Components Center

Medtronic Energy and Components Center, 6800 Shingle Creek Parkway, Brooklyn Center,
MN 55430

T: (001)(763) 514 0926; F: (001)(763) 514 0899; e-mail: joachim.hossick-schott@medtronic.com

Abstract

Electrochemical reactions promoting the generation of electronic charge are expected at electrified metal-oxide-electrolyte interfaces. Subsequently, this charge may be injected into the oxide layer and transfer across to the substrate metal. One such reaction, the oxidation of acetic acid at the charged tantalum-pentoxide-electrolyte interface, is addressed in this paper. Isotopic substitution experiments involved the replacement of the ^{12}C atom in the carboxyl-group of the acetic acid molecule by its ^{13}C isotope. The subsequent detection of the ^{13}C isotope in dissolved CO_2 gas demonstrates the oxidation. The CO_2 molecule-yield per electronic unit charge is estimated to be in the range of 5%. The proposed reaction at the electrified interface resembles the classic Kolbe reaction. Likely sites of the reaction may be flaws in the amorphous tantalum pentoxide.

Introduction

Implantable cardioverter-defibrillators are designed to restore a normal heart rhythm by providing life-saving electrical pulse therapies. Upon detection of ventricular fibrillation, a set of high-voltage capacitors is charged to a potential between 600 and 800 V. A therapeutic pulse carrying about 10 – 40 J of energy is generated by discharging the capacitors directly in the patient heart tissue. Electrolytic capacitors are used exclusively inside these devices. The high voltage capacitor assembly, a primary battery and a hybrid circuit board constitute the three main parts within an implantable defibrillator. Breyen et al. discussed the requirements for defibrillation capacitors in a previous CARTS publication (1). The battery typically stores energy sufficient for about 150 therapeutic pulses over a device life time as long as 10 years. During this entire time, the capacitor has to be operational. Hence, high-voltage capacitor technology is of paramount importance for enabling this life-preserving therapy. Two liquid electrolyte capacitor technologies are currently used in the implantable defibrillator industry, one based upon etched and stacked Al plates (1,2), the other upon pressed and sintered Ta powder (3,4) as anode materials. Anodically grown oxides constitute the dielectric layer on both, Ta and Al anode materials. This paper will focus specifically on anodized Ta surfaces.

The formation of the anodic tantalum pentoxide is usually carried out in a forming electrolyte specifically designed to yield a high quality oxide. The process was studied in great detail during the 1930's by Güntherschulze and Betz (5), and later by Young (6). Numerous formulations of such forming electrolytes exist today. Some of the more advanced forming electrolytes were formulated and discussed by Melody and Chavez (7). After formation, the Ta anode is typically immersed into a different electrolyte, the so-called working electrolyte.

This electrolyte is used during operation of the capacitor. In order to keep the capacitors' equivalent series resistance (ESR) low, the working electrolyte is typically one to two orders of magnitude more conductive than the formation electrolyte. Empirical data suggest a proportional relationship between the leakage current and the conductivity of the working electrolyte (8). A small amount of leakage current must be tolerated in all capacitor applications.

The electrolyte is the source for the electronic charge that constitutes the leakage current. In aqueous electrolytes, OH^- anions are the likely charge donors (9). However, other electrolyte constituents electrochemically reacting at the charged oxide-electrolyte interface may also contribute. This paper demonstrates that the oxidation of acetic acid at the tantalum pentoxide – electrolyte interface is one such contributing reaction.

Charge transfer at electrode-electrolyte interfaces

a.) Metal-oxide-electrolyte interfaces in capacitors

Charge transport across the oxide layer may be electronic or ionic in nature. Electronic charge transport may be initiated by electrons emitted from impurities in the oxide or from electrochemical reactions at the oxide-electrolyte interface; both electron sources could influence each other. Ionic charge transport occurs mainly during formation of the oxide: here, it is a necessary prerequisite for oxide growth. In contrast, any kind of charge transfer across the oxide is undesirable on pre-existing anodic oxide films immersed in a working electrolyte. Practically, however, there is a small amount of electronic charge transport from the working electrolyte through the oxide and into the substrate metal, specifically at high potentials.

Upon immersing the capacitor anode into the working electrolyte solution, the electrochemical double layer establishes itself at the oxide-electrolyte interface, as sketched in Figure 1. At potentials far below the formation potential of the anodic oxide (Figure 1, left), water molecules reorient in the vicinity of the surface and solvated anions – in aqueous electrolytes mainly OH^- – migrate to the interface and may adsorb there (10). According to Malinenko et al. (11), at low to medium-high potentials up to about 50 % of the formation potential, a small amount of charge may transfer across the electrolyte-oxide interface in cracks and faults (Figure 1, center). In this potential range, the current-voltage trace should be largely linear or ohmic (11). Upon increasing the potential further towards about 85% of the oxide formation potential, the rate of electrochemical reactions at the interface will increase (11, 12). In turn, charge transport across the oxide will increase (Figure 1, right).

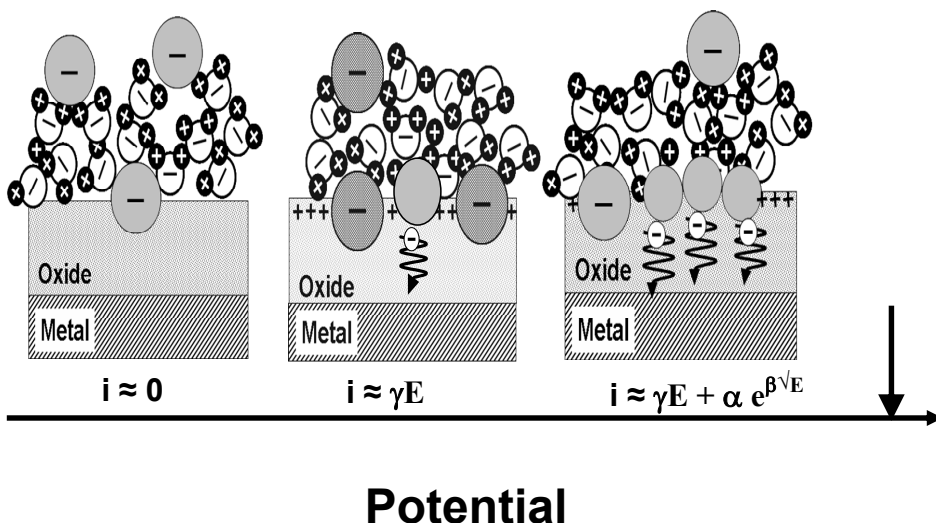


Fig. 1. Sketches of the charged oxide-electrolyte interface. With increasing potential, water molecules reorient and more and more anions become specifically adsorbed (chemisorbed), some charge transfer may occur through cracks and crevices in the oxide (center). Increasing the potential further towards the formation potential causes transport of electronic charge emitted by discharge reactions in the interfacial region (right). The contributions to the current i in the respective potential ranges are indicated based on equation [1] (see text below).

Disregarding breakdown phenomena, Malinenko et al. (11) and Odynets and Chekmasova (12) concluded that the measured current across the metal-oxide-electrolyte interface will be predominantly electronic in the entire potential range up to about 85 % of the formation potential. Ionic motion becomes more significant only at or just below the formation potential. Overall, three contributions are expected to the current measured in the entire potential range up to the formation potential (11):

$$i = \gamma E + \alpha e^{\beta \sqrt{E}} + A e^{BE} \quad [1]$$

In equation [1], i is the overall current passing through the metal-oxide-electrolyte interfaces, α , A , β , B and γ are constants, and E is the electric field. Only the first two terms of equation [1], γE and $\alpha e^{\beta \sqrt{E}}$ are relevant for this paper, as they describe the electronic contribution to the overall current. The term $A e^{BE}$ describes the ionic contribution.

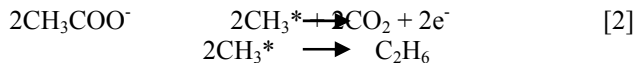
In aqueous electrolytes, electrons injected into the oxide layer are mostly generated by the oxidation of chemisorbed OH^- groups (12). However, other electron sources, such as impurities embedded in the oxide have been experimentally verified: Klein and Jaeger (13) deposited monolayer quantities of Fe_2O_3 and other transition metal oxides on the Ta_2O_5 anodic oxide surface, thus simulating a massive contamination of the oxide with impurities. Upon charging the interface in a supporting electrolyte, these authors could demonstrate

electron emission from the transition metal layer into the substrate metal via charge transport across the oxide. Charlesby (14) and Smith (15) demonstrated on Al₂O₃ coated electrodes that the electrolyte composition decisively influences the electronic charge transport across the oxide. Later, Ikonopisov and Elenkov (16) did show that the same holds true for Ta₂O₅ and Nb₂O₅ electrodes.

So far, breakdown phenomena have not been discussed in this overview. However, operating a capacitor at potentials close to the formation potential in a high conductivity working electrolyte may, of course, increase the probability for breakdown of the oxide-electrolyte system. A general account of breakdown phenomena in thin films was given by Klein (17). Breakdown mechanisms specifically in Ta₂O₅ -and related oxide-electrolyte systems were reviewed by Albella et al. (18) and more recently again by Simkins (19) et al. It is generally accepted that the breakdown of the electrolyte-oxide system is based upon an avalanche-type process: briefly, electronic charge is accelerated in the extremely high electric field of several MV/cm at the metal-oxide-electrolyte interface. Secondary electrons are emitted upon impact of the primary charge, generating an avalanche multiplying in strength as it travels across the oxide layer.

b.) The decomposition of acetic acid in aqueous electrolytes

One specific electrolysis reaction producing electronic charge at electrode-electrolyte interfaces is the oxidation of acetic acid. The oxidation occurs on charged electrodes in aqueous electrolyte and constitutes one of the more popular electrolysis reactions in electrochemistry. First discovered by Faraday in 1834 (20) and later investigated in more detail by Kolbe (21), this reaction is described as follows:



Reviews on the Kolbe reaction were given by Vijh and Conway (22) and more recently again by Grinberg and Vassiliev (23). Most of the vast amount of work that was done to understand this reaction was performed using Pt electrodes. Even on this one particular electrode, many variations of reaction [2] are documented. For example, it is commonly assumed that oxidation of the electrode substrate energetically precedes the electrolysis of the acetate; that is, the onset of the acetate decomposition is measured at higher electrode potentials than the substrate oxidation. Koch and Woods (24), however, found that at potentials below the oxidation of Pt, a complete oxidation of aqueous acetate to carbon dioxide and water appears to be possible, because no reaction products other than CO₂ were detected in their experiment. Other important variations of reaction [2] include the increasing formation of methane at the expense of ethane with decreasing current densities (25) and the production of methyl acetate instead of methane or ethane (26). Methane, ethane and methyl acetate are evidently only some of the possible reaction products of the CH₃* radical. Clearly, the radical is the “wild card” in the Kolbe-type reactions. Depending upon the oxide- and electrolyte constituents, any number of reactions appears possible.

CO₂ is produced in all known variations of reaction [2] in aqueous electrolytes. The molecule dissolves readily in water and in many polar, organic solvents (27). As will become apparent below, it is this property that eases its qualitative detection on the one hand and complicates the quantitative measurement on the other.

Experimental Section

Capacitor test cells were constructed as described previously (28). Briefly, a porous, sintered tantalum anode slug was inserted into a titanium case, as sketched in Figure 2. Bare and graphite-coated Ti surfaces were used as cathodes (29). The anode slugs were anodized in a forming electrolyte capable of producing oxides with a thickness in excess of 0.4 μm . The capacitors were filled with a working electrolyte containing water, an organic solvent, a salt and about 10 % w/w of glacial acetic acid. Glacial acetic acid containing isotopically pure ^{13}C carboxylate was obtained from Aldrich and used as received. At a temperature of 37 $^{\circ}\text{C}$, some of the test cells were charged once to a target potential in the range above 150 V and held there for up to 120 minutes. With other cells, the potential was cycled between 0 V and the target potential for 350 times. A charging current of 10 mA was used in all cases.

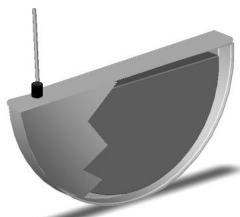


Fig. 2. Sketch of the Ta slug capacitor

Upon completion of the hold time or the potential cycling, the electrolyte or the headspace gas formed in the test cell were analyzed. For the electrolyte analysis, a small hole was punched into the Ti case, enabling a syringe to extract a defined volume of electrolyte from the test cell. The extracted electrolyte sample was then injected into the fill-port of a HP 5890A GC+5970 MS system, which is a gas chromatograph interfaced with a mass spectrometer. The instrument was used in a mass-selective thermal desorption spectroscopy mode; that is, the analyte was heated and its vaporized components were directly analyzed and recorded using only the mass spectrometer of the instrument. In determining the relative amount of masses 44 ($^{12}\text{CO}_2$) and 45 ($^{13}\text{CO}_2$) desorbing from the analyte, the fragmentation pattern was recorded in order to ensure positive identification of the molecules. The absolute amount of CO_2 dissolved in the analyte was estimated using a method suggested by Che and Ilmberger (30), who related the conductivity L of an aqueous solution of CO_2 directly to the concentration $[\text{CO}_{2(\text{aq})}]$:

$$L = 8.18[\text{CO}_{2(\text{aq})}]^{0.5} \mu\text{S cm}^{-1} \quad [3]$$

Hence, a sample of DI water was enriched with CO_2 and its conductivity measured. Then, the mass spectroscopic peak height of this sample could be compared to the CO_2 peak height obtained from the desorption spectra of the test cell electrolyte. This method only yields approximate results: Some of the CO_2 likely escapes upon opening the hermetically sealed test cell, just as it does upon opening a bottle of carbonated water. In addition, about 15 % of the dissolved CO_2 will react with water to become carbonate (30), and CO_2 desorption from water in the control sample imperfectly simulates desorption from the electrolyte matrix.

Gas chromatography / mass spectroscopy (GC/MS) was also used for head space gas analysis. A hole was punched into the Ti case in a small evacuated chamber. Gases were extracted from the chamber using a gas tight syringe and injected into the fill port of the chromatograph. Again, this method yields only approximate results as some of the CO_2 will remain dissolved in the electrolyte.

Results and Discussion

a.) The generation of CO₂ at the charged oxide-electrolyte interface

Figure 3 shows the relative amount of dissolved CO₂ observed in the test cell electrolyte upon increasing the hold time at target potential. Repeating the same experiment for one of the time points with electrolyte, in which the isotope ¹³C substituted the ¹²C atom in the

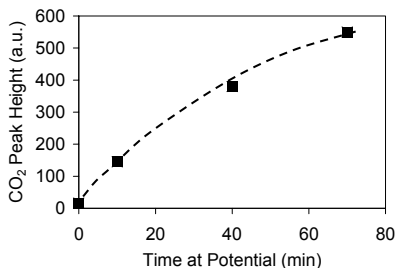


Fig. 3. The relative amount of CO₂ in liquid electrolyte samples drawn from test cells, which were held at potential for various times at 37 °C.

carboxylic group revealed the production of pure ¹³CO₂. No ¹²CO₂ was observed within the detection limits of the measurement. Therefore, the CO₂ signal clearly originates from the oxidation of the carboxylic group in the acetic acid molecule, not from any other electrolyte species. In all likelihood, the reaction occurs at the tantalum pentoxide-electrolyte interface at the anode of the test cell, as the electrolysis reaction [2] is an oxidative process. Calibrating the CO₂ signal as described above and normalizing it to the amount of leakage charge passed through the capacitor reveals a CO₂-molecule yield per electronic elementary charge of about 5 % for the

exposure time range 10 – 40 minutes. For longer exposures, this yield appears to decrease to less than 1 %. The electrochemistry behind this decline will be the subject of a future publication.

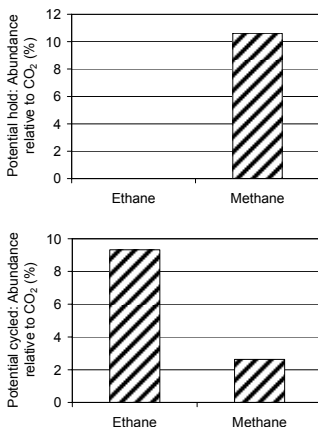


Fig. 4. The abundance of ethane and methane relative to the abundance of CO₂. Top: Charge and hold experiment. Bottom: Potential cycling.

Figure 4 illustrates that only trace amounts of ethane and methane are detectable in head space gas analysis. The abundance of ethane and methane in the head space gas is at most about 10 % of the CO₂ abundance in the head space. Furthermore, Figure 4 demonstrates that after potential-hold experiments, in which only a small leakage current flows, ethane is not detectable; only methane is observed in the head space gas (Figure 4, left). However, during potential cycling, where a charging current of 10 mA flows repeatedly, the production of ethane appears actually favored over that of methane (Figure 4, right). Clusius and Schanzer (25) observed a similar phenomenon in their study upon the variation of the current density. They argued that ethane production is a function of the surface density of the methyl radical. Under high density conditions, ethane is formed; low densities will favor methane. This likely is the explanation for the results shown in Figure 4.

Therefore, we conclude that a Kolbe-type reaction as sketched in Figure 5 does occur on the Ta₂O₅ surface. However, only about 10 % of the reaction products of the CH₃* radical have been identified directly in this study. Therefore, some other reaction mechanism must be at work, possibly the production of methyl acetate given by Vijn (26).

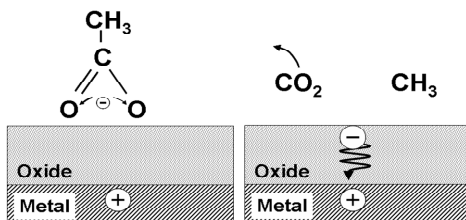


Figure 5. Sketch of the decay of acetic acid at the charged oxide-electrolyte interface. Left: chemisorbed acetic acid anion. Right: carbon dioxide emission and charge injection into the oxide after the oxidation of the anion.

b.) Possible reaction sites

Reaction [2] is likely tied to oxide surface sites where elevated local potentials or elevated local leakage currents are encountered. Examples for such sites are pin holes, thin spots induced by, for example, carbon contamination and crystalline areas within the otherwise amorphous oxide. Many researchers have studied these crystalline areas (see, e.g., refs. 31-34), as their growth could degrade the performance of Ta capacitors severely. These crystalline oxide areas promote a localized increase in leakage current density (31).

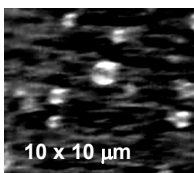


Figure 6. Bubbles formed on a charged Ta₂O₅ surface with a high density of crystalline sites. Anodized Ta sheet metal was used in this experiment.

Therefore, a crystalline site may act as a funnel for electronic charges produced by charge-generating oxidation reactions such as the oxidation of chemisorbed OH⁻ anions described by Odynets (9) or the oxidation of acetic acid described in this paper. Increased local charge transport will heat the oxide up, causing gaseous reaction products or electrolyte vapor to form above the crystalline site. As demonstrated in Figure 6, bubbles are indeed observed upon charging Ta₂O₅ coated sheet-metal surfaces with a high density of crystalline sites. However, the chemical identity of the species inside the bubbles is unclear; oxygen, carbon dioxide and electrolyte vapor are possible constituents. It is plausible that the elevated temperatures produced upon charging the crystalline sites would also enhance reaction [2]. Indeed, the higher the temperature of the electrode-electrolyte system, the lower the potential needed to initiate the reaction (35). Therefore, crystalline sites may be expected to play a role in the generation of CO₂ on the Ta₂O₅ surface.

Conclusions

Acetic acid decomposes on the electrified Ta₂O₅ surface into CO₂ and other reaction products such as C₂H₆ and CH₄. The reaction likely resembles a variation of the classic Kolbe reaction. The electronic charges produced upon the decay of the acetic acid molecules are the source for up to 5% of the total leakage current of the capacitor. Crystalline areas in the otherwise amorphous Ta₂O₅ surface, pinholes and thin spots in the oxide are discussed as the possible sites for the Kolbe reaction to take place.

References

- (1) M. Breyen, A. Rorvick, P. Skarstad, 22nd Capacitor and Resistor Technology Symposium (CARTS USA), 197, (2002).

- (2) J.L. Stevens, M.A. Moore, X. Jiang, C.R. Feger and T.F. Strange, Capacitor and Resistor Technology Symposium (CARTS USA), Proceedings, pp. 249 – 254, (2004).
- (3) D. A. Evans, US Patent #5,369,547 (1994).
- (4) A. Shah, B.C. Muffeletto, N.N. Nesselbeck, US Patent 5,894,403 (1999).
- (5) “Elektrolyt-Kondensatoren”, A. Günther-schulze, H. Betz, M. Krayn publisher, Berlin, 1937.
- (6) “Anodic oxide films”, L. Young, Academic Press, London, New York, 1961.
- (7) B.J. Melody, B. Chavez, 12th Capacitor and Resistor Symposium (CARTS USA), (1992)
- (8) I. Montero, J.M. Alebella, and J.M. Martinez-Duart, J. Electrochem. Soc., 132(4), 814 (1985).
- (9) L.L. Odynets, Materials Science Forum, 185-188, pp. 553-562 (1995).
- (10) “Modern Electrochemistry”, Vol. 2, p. 845 ff, J.O’M. Bockris, A.K.N. Reddy, Plenum Press, New York (1970).
- (11) V.P. Malinenko, L.L. Odynets, S.S. Chekmasova and E. Ya. Khanina, Russian Journal of Electrochemistry, 7 (12), pp. 1846 – 1848 (1971).
- (12) L.L. Odynets and S.S. Chekmasova, Russian Journal of Electrochemistry, 9(8), pp. 1177-1180 (1973).
- (13) G.P. Klein and N.I. Jaeger, J. Electrochem. Soc., 117, 1483 (1970)
- (14) A. Charlesby, Proc. Phys. Soc., 66, 533 (1953).
- (15) A.V. Smith, Can. J. Phys., 37, 591 (1959).
- (16) S. Ikonopisov, N. Elenkov, J. Electroanal. Chem., 86, pp. 105-114 (1978)
- (17) N. Klein, Advances in Physics, 21, 605 (1972)..
- (18) J.M. Albella, I. Montero, J.M. Matrtinez-Duart, V. Parkhutik, J. Mat. Sci., 26, 3422, (1991).
- (19) L.F. Simkins, K.B. Doyle and T.B. Tripp, 22nd Capacitor and Resistor Technology Symposium (CARTS USA), pp. 236-43 (2002).
- (20) M. Faraday, Pogg. Ann. (Annalen der Physik und Chemie), 33, 438 (1834).
- (21) H. Kolbe, Ann. Chim. Phys., 69, 257 (1849).
- (22) A.K. Vijh and B.E. Conway, Chemical Reviews, 67(6), pp. 623 – 664 (1967)
- (23) V.A. Grinberg and Yu. B. Vassiliev, Russian Journal of Electrochemistry, 32(3), pp. 281-303 (1996).
- (24) D.A. Koch and R. Woods, Electrochimica Acta, 13, pp. 2101 – 2109 (1968).
- (25) K. Clusius und W. Schanzer, Z. Physikal. Chem., 192 (5/6), pp. 273 – 291 (1943).
- (26) A.K. Vijh, J. Electrochem. Soc., 119(6), pp. 679 – 683 (1972).
- (27) A. Henni, A.E. Mather, J. Can. Petrol. Technol., 38(13), pp. 1 – 7 (1999).
- (28) J. Hossick Schott, Capacitor and Resistor Symposium (CARTS-Europe), Proceedings, pp. 157 – 165 (2004).
- (29) J. Hossick Schott, 26th Capacitor and resistor Symposium (CARTS-USA), Proceedings, pp. 261 – 267 (2006).
- (30) G. Che and Johann Ilmberger, American Society of Limnology and Oceanography (ASLO) Journal, 39(4), pp. 976 – 981 (1994).
- (31) N.F. Jackson, J. Applied Electrochem., 3, pp 91 – 98, (1973).
- (32) Y. Pozdeev-Freeman, A. Gladkikh, J. Elect. Mat. 30(8), pp. 931 – 936 (2001).
- (33) B. Melody and T. Kinard, J. Electrochem. Soc., 140(11), L162 (1993).
- (34) J. Hossick Schott and A. Belu, 17th Capacitor and Resistor Conference (CARTS Europe), Proceedings, P. 103 (2003).
- (35) G. Belanger, C. Lamarre, and A.K. Vijh, J. Electrochem. Soc., 122(1), pp. 46 – 50 (1975).